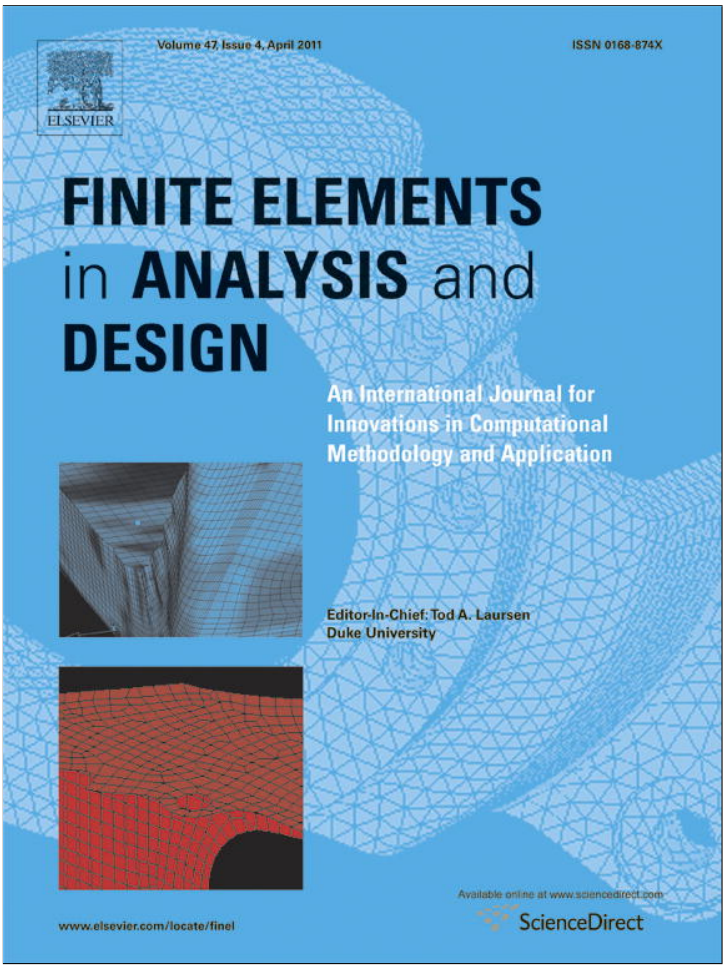

Finite Elements in Analysis and Design 47 (2011) 413–423

Contents lists available at ScienceDirect

Finite Elements in Analysis and Design

journal homepage: www.elsevier.com/locate/finel

Design optimization of spot-welded plates for maximum fatigue life

Ahmet H. Ertas [a], Fazıl O. Sonmez [b,*]

[a] Department of Mechanical Engineering, Karabuk University, Karabuk, 78050, Turkiye
[b] Department of Mechanical Engineering, Bogazici University, Istanbul, Bebek, 34342, Turkiye

ARTICLE INFO

Article history:
Received 27 August 2009
Received in revised form
21 July 2010
Accepted 17 November 2010
Available online 6 January 2011

Keywords:
Spot weld
Structural Optimization
Fatigue life prediction
Finite element analysis
Nelder-Mead

ABSTRACT

Resistance spot welding is the most preferred and widely used method for joining metal sheets in automotive and many other industrial assembly operations. Spot-welded joints are usually the weakest parts of structures leading to fatigue failure under fluctuating loads. Increasing the fatigue strength of the joints through geometrical changes will also increase the overall integrity of the whole structure.

In this study, a methodology is proposed to find the optimum locations of spot welds and the optimum overlapping length of the joined plates for maximum fatigue life. Minimum weld-to-weld and weld-to-edge distances recommended by the industry are considered as side constraints. The total strain life equation is used to predict the fatigue life. In order to use this model, the strain state in the structure developed under cyclic loading is required. For this purpose, a nonlinear finite element analysis is carried out, taking into account residual stresses due to localized plastic deformations around the spots. Nelder-Mead (Sequential Simplex) is employed as the search algorithm in the optimization procedure. A number of problems are solved to demonstrate the effectiveness of the proposed method.

1. Introduction

Automotive bodies as many other structures are composed of metal sheets joined by spot welds. A spot weld is materialized by clamping the sheets with two pincers while applying force and transmitting current as depicted in Fig. 1. The electrical resistance of the contacting sheets generates sufficient heat at the faying surfaces to melt the metal; eventually a nugget develops and the interface locally disappears.

Because spot weld joints provide localized connection, and thus lead to high stress concentration in the joined plates, any improper design may result in excessively high stresses and premature failure. The critical failure mode under fluctuating loads is mainly fatigue. Knowing that fatigue crack initiation is very sensitive to stress level, that means increase in stress level dramatically increases the likelihood of fatigue failure, designers may significantly boost fatigue strength of a component by introducing changes in its geometry that will reduce the level of stress in highly stressed regions. The geometry and material of a joint can be tailored to obtain optimal performance and the most effective use of material. The design variables for spot welded structures are locations of spot welds, length of the overlapping portion of plates, material, plate thickness, diameter and number of the spot welds. The effects of spot-weld diameter, sheet thickness and joint type as exemplified in tensile shear (TS), modified tensile shear (MTS), coach peel (CP), and modified coach peel (MCP) specimens were investigated in the previous study conducted by the authors [1]. Because a small spot weld cannot be produced through thick sheets, or thin sheets cannot be joined by large spot welds, i.e. the range of feasible spot weld diameters for a given sheet thickness is limited, a parametric study like the previous one [1] is sufficient to determine their effects and optimal values. In this study, positions of spot welds and overlapping length of the plates are considered as design variables to maximize the fatigue life. Because, there are quite a large number of possible configurations, use of an optimization algorithm is necessary to find the optimal design. Sheet thickness and material are assumed to be predetermined according to the strength requirements of the structure. The diameter of the spots, d, is chosen based on an empirical formula recommended by the American Welding Society (AWS), Society of Automotive Engineering (SAE), and the American National Standards Institute (ANSI) [2] given as

$$d = 4\sqrt{t} \tag{1}$$

where d and t are the weld-nugget diameter and sheet thickness, respectively (in mm). The number of spots is not chosen as an optimization variable. However, the optimization process is repeated for different numbers of spots and its effect on the optimal performance is determined.

In the literature, there are few studies about optimization of spot-welded structures. Zhang and Taylor [3] optimized the positions of two spot welds in a tensile shear specimen. They formulated two optimization problems: one was to maximize the stiffness of the structure under fatigue life constraints and the other was to seek the

* Corresponding author. Tel.: +90 212 359 7196; fax: +90 212 287 2456.
E-mail address: sonmezfa@boun.edu.tr (F.O. Sonmez).

0168-874X/$ - see front matter © 2010 Elsevier B.V. All rights reserved.
doi:10.1016/j.finel.2010.11.003

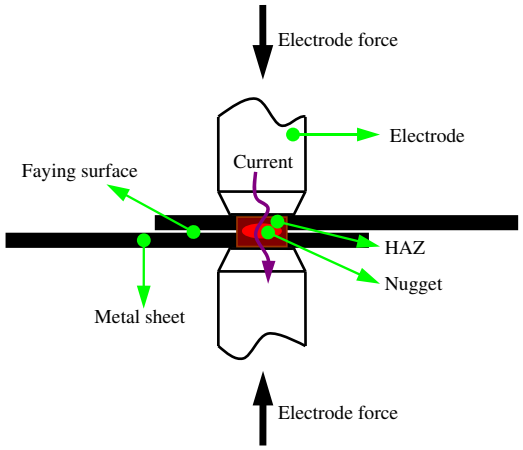

Fig. 1. A scheme of the resistance spot welding process.

maximum fatigue life of the structure. The fatigue life was not directly maximized. The objective function to be minimized was the maximum radial stress, which was assumed to be correlated with the fatigue life. Chae et al. [4] investigated optimal spot welding locations of spot welds under static and impact loading to maximize safety factors of spot welds. Rui et al. [5] used an optimization algorithm to minimize the stress intensity factor of spot welds, which was assumed to be a control parameter for the fatigue life of the structure. Finally, Liangheng et al. [6] proposed a method to reduce the number of welds in automobile bodies subject to rigidity requirements.

In the present optimization procedure, the fatigue life is directly calculated and maximized as opposed to the previous studies. In design optimization, in order to avoid false optimum designs, the objective function, in this case the fatigue life, should accurately be calculated. Because of high stress concentration, nonlinear and plastic deformation is likely to occur around the welds even at low load levels. These stresses control the failure life of the joint and thus the whole structure. Strain based models are known to better assess fatigue life of plastically deformed parts. Accordingly, the total strain life equation (or the modified Coffin-Manson equation) was used, which was observed [1,7] to be better in predicting fatigue life of spot welded joints in comparison to other strain based models. In addition to choosing a reliable fatigue assessment model, another requirement for accurate predictions is to correctly determine the change in the strain state under cyclic loading. For this purpose, a nonlinear finite element analysis was carried out using nonlinear material properties and contact elements on the inner surfaces of the plates. Plastic deformations induced during loading and residual stresses developed after unloading were taken into account. The fatigue assessment model and FE model were verified before [1,7] by comparing the predictions with the experimental data for various types of spot welded structures and for different ranges of loads.

It should be noted that processing parameters like welding current, welding time, clamping force, electrode diameter, hold time and process conditions like clamping conditions, welding sequence have significant effect on the quality of the spot-weld joint in terms of fatigue strength and geometric distortions. In order to ensure the integrity of the joint, one should therefore consider these factors. However, the present study focuses only on design optimization; optimum selection of processing parameters is outside the scope of this study.

2. Fatigue life prediction model

Fig. 2 shows the loading on a spot-weld joint. Due to the eccentricity, the plates are bent, and tensile stresses develop at the inner surfaces.

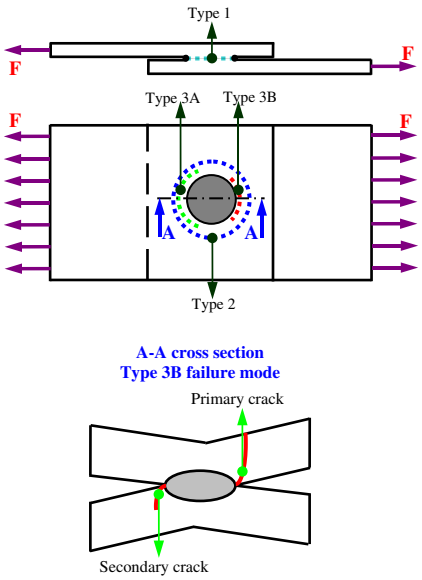

Fig. 2. Depiction of the failure modes observed in spot welded joints [7].

Besides, due to the high stress concentration, plastic deformation is likely to occur around the welds. After unloading compressive residual stresses may develop at these locations. For these reasons, the stresses around the nugget control the useful life of the joint and thus the specimen. There are mainly four failure modes for spot welded joints. These are weld-interfacial failure mode, the sheet-tearing mode through width, the sheet-tearing mode through thickness and the nugget-pull-out mode [7–14]. In weld-interface failure mode (shown in Fig. 2 as type-1), a fracture occurs parallel to the sheets due to poor welding or small weld - diameter - to - sheet - thickness ratio. In the nugget - pull - out mode (shown in Fig. 2 as type-2), the weld is pulled out of one of the sheets. Under fluctuating loads, fatigue failure is most likely to happen, which starts with the initiation of a crack in a highly stressed region near the nugget. Once a crack develops, one of two things may happen. If the load is sufficiently small, the crack initiates at some distance away from the nugget and then propagates around the nugget to a large width before propagating through the thickness. This type of failure mode is called the sheet - tearing mode through width (shown in Fig. 2 as type-3A). This type of failure is very common for the chosen load ranges. However, if the load is high, the crack initiates closer to the nugget and propagates through the thickness without becoming wide. This is called the sheet - tearing mode through thickness (shown in Fig. 2 as type-3B) [7].

In order to be able to correctly predict the fatigue damage for such a complex stress state one should use a reliable fatigue assessment model. The fatigue life models are classified as strain-based and stress-based approaches in general. The authors examined both stress-based and strain-based approaches and the predictions of stress-based approaches were found to be overly conservative for spot weld joints [7], which might be due to highly localized plastic deformation around the spot weld nuggets. On the other hand, strain-based approaches showed a better correlation with the experimental data. Among them the total strain life equation, which is actually Coffin-Manson equation modified by including the effect of elastic strain, yielded the best predictions. Hence in this study, this equation was used for fatigue life assessment. This model relates alternating true elastic and plastic strains, $\Delta\varepsilon_e$ and $\Delta\varepsilon_p$, to number of cycles (N_f) to failure, as follows [15,16]:

$$\frac{\Delta\varepsilon}{2} = \frac{\sigma_f'}{E}(2N_f)^b + \varepsilon_f'(2N_f)^c \tag{2}$$

where σ_f' is the fatigue strength coefficient, ε_f' is the fatigue ductility coefficient, b is the fatigue strength exponent, and c is the fatigue ductility exponent, which are empirically determined material constants.

The state of stress at the peripheries of spots is multiaxial even if the plates joined by spot welds are subjected to uniaxial in-plane loads. Because the fatigue assessment model is appropriate for uniaxial stress states, an equivalent uniaxial alternating strain, ε_{qa}, is calculated, which leads to the same fatigue life. In the previous study [7], octahedral shear strain was found to better reflect the effect of multiaxial strain state around the spot welds.

$$\varepsilon_{qa} = \frac{\sqrt{(\varepsilon_{a1}-\varepsilon_{a2})^2+(\varepsilon_{a2}-\varepsilon_{a3})^2+(\varepsilon_{a3}-\varepsilon_{a1})^2}}{\sqrt{2}(1+\nu)} \tag{3}$$

where ε_{a1}, ε_{a2}, and ε_{a3} are the principal alternating strains.

2.1. Comparison of the predicted and measured fatigue lives

The accuracy of the fatigue life prediction method used in this study was verified by comparing the predictions with the fatigue lives of modified coach peel (MCP) and modified tensile shear (MTS) specimens experimentally obtained by Pan [10,17] and Ertas et al. [1,7]. The FE calculations were carried out using the material properties, loading, and geometry of the specimens provided in those studies. The tested specimens were made of two different types of low carbon steels. In MTS specimens, the weld nugget was basically subjected to shearing force. On the other hand, in MCP specimens, the spot weld was subjected to an out-of-plane separating force. Comparisons were made for different load ranges. Fatigue lives were predicted using the total strain life equation. As seen in Figs. 3–5, the results compare quite well. The good correlation obtained between the predictions and the measured data for different specimen and weld geometries, loading cases, load fluctuations, and materials imparts confidence on the accuracy of the FE analysis and the fatigue assessment model for the spot-weld joints.

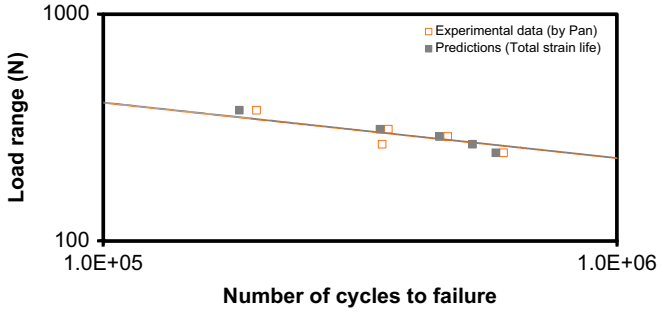

Fig. 3. Comparison of the predicted fatigue lives with the experimental results obtained by Pan [10] for MCP specimens.

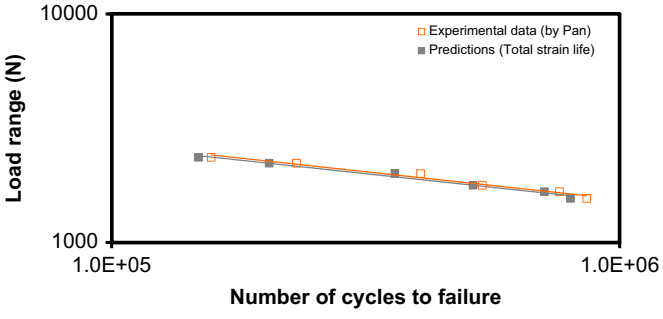

Fig. 4. Comparison of the predicted fatigue lives with the experimental results obtained by Pan [10] for MTS specimens.

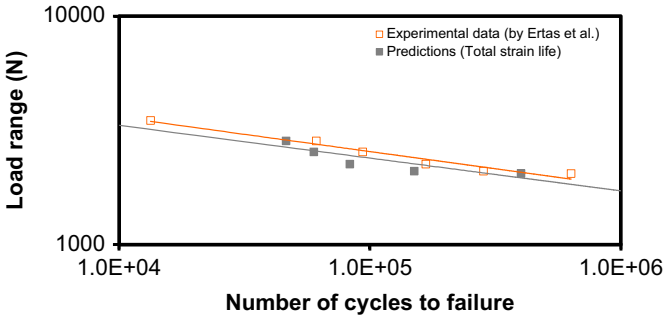

Fig. 5. Comparison of the predicted fatigue lives with the experimental results obtained by Ertas et al. [1,7] for MTS specimens.

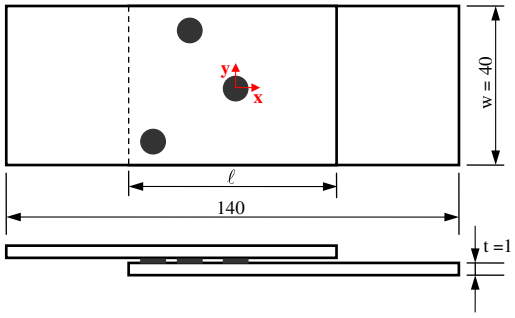

Fig. 6. Geometry of the joint with three spot welds (top and side views).

3. Problem statement

In this study, a common geometry, tensile-shear (TS) joint with two or three spot welds (Fig. 6), was considered and optimized for various in-plane loads. The variables of the design optimization process were chosen to be the x and y coordinates of the spot welds, x_i, y_i, and the length of the contacting surface between the joined metal sheets, ℓ. The origin of the coordinate axes was taken to be the center of the overlapping region. The spot weld diameter, d, metal sheet thickness, t, and width of the plate, w, were predetermined to be 4, 1, and 40 mm, respectively,

The main objective of the design optimization problem is to maximize the fatigue life, $2N_f$, of the joint.

$$\text{Maximize } N_f \tag{4}$$

The design variables are subject to a number of side constraints. The spot welds should be prevented from interfering with each other and getting close to the boundaries of the sheets; this means that the design should conform to the standards related to weld-to-weld spacing and weld-to-edge distance. According to industrial organizations like Precision Metalforming Association (PMA) and American Welding Society (AWS) the distance between an edge and the center of a spot weld should be greater than one spot weld diameter, d. Accordingly, the constraint equations are given as

$$-(\ell/2-d) \le x_i \le \ell/2-d \tag{5}$$

$$-(w/2-d) \le y_i \le w/2-d \tag{6}$$

Besides, the distance between the centers of the spot welds should be greater than twice the spot weld diameter as recommended by the industry. Then,

$$s_{ij} > 2d \tag{7}$$

where s_{ij} is the distance between spot welds i and j.

4. Methodology

4.1. Objective function

In the standard form, the objective function is constructed so as to minimize its value. The main objective in this study, on the other hand, is to maximize the fatigue life. For this reason, negative of fatigue life, $-N_f$, appears in the objective function to be minimized. In the design of spot-welded joints, there is uncertainty regarding the proper value of the overlapping length, ℓ. Small lengths will be restrictive for optimization; choosing large lengths will be against the effective use of material. For these reasons, ℓ is incorporated into the objective function. While it is minimized, ℓ will also be decreased. In the optimization procedure, external penalty functions are used to transform the constrained optimization problem into an unconstrained one for which the chosen search algorithm is suitable. If the value of a design variable is outside its feasible range, a penalty value is calculated and added to the value of the objective function. The objective function to be minimized then becomes

$$f_{obj} = c_1 \frac{\ell}{w} - c_2 \frac{N_f}{N_r} + c_3 \sum_i P_i \tag{8}$$

where N_r is the reference life used to normalize the fatigue life, N_f. N_r is taken to be 10^6 cycles, which is the limit for the infinite life for steels. c_i are suitable coefficients ($c_1=0.01, c_2=1, c_3=10$), and P_i are penalty values. The overlapping length, ℓ, was normalized by the width of the plates. In this way, the fatigue life is maximized with an effective use of material. Because the main objective is to maximize the fatigue life, N_f, the factor of N_f, c_2, is chosen to be much larger than the factor c_1. In this way, material use is not reduced at the expense of fatigue strength. x and y coordinates of the spot welds should satisfy the constraints given in Eqs. (5)–(7). Consider that the constraint equations (Eqs. (5)–(7)) are written in the standard form as

$$g_k(\boldsymbol{x},\boldsymbol{y},\ell) \geq 0 \tag{9}$$

If kth constraint takes a negative value, i.e. if it is violated, a penalty term, P_k, is calculated using the following equation:

$$P_k = -g_k \quad \text{if } g_k < 0 \tag{10}$$

If the constraint is satisfied, its corresponding penalty value is set equal to zero.

$$P_k = 0 \quad \text{if } g_k \geq 0 \tag{11}$$

The coefficient of the penalty functions, c_3, is equal to 10. This is sufficiently high to direct the search into the feasible domain considering that stresses get larger as a spot weld comes close to the border leading to decrease in fatigue life and increase in the objective function value. This means that if a constraint is violated, apart from penalty values, the other terms of the objective function are also expected to increase. Therefore with the addition of the penalty value, the optimization is definitely prevented from converging inside the infeasible domain.

4.2. Optimization algorithm

In optimization problems one may use zero, first or second order search algorithms [18,19]. Considering that the value of the objective function in the present problem is numerically calculated using FE method, calculating its first or second order derivatives may pose difficulties. During structural design optimization, such geometrical changes may be introduced that finite element analysis may fail, e.g. geometry may not be created because connectivity is lost, for example spot welds go outside the plates in the present problem, or the search algorithm may generate negative values for dimensions, or the geometry may become so complex that finite element mesh cannot be generated, e.g. spot welds may come very close to each other. In these cases, a large penalty value is assigned to the objective function. At that rate, however, calculating the sensitivities is not possible because if the values of the design parameters are changed by small steps, the same objective function value, which is the assigned penalty value, is obtained. In the case of non-differentiable and discontinuous objective functions, either some special constraints are introduced or user intervention is needed. For this reason, use of a high order search algorithm is not preferred in this study. Although zero order algorithms are computationally less efficient in comparison to first or second order algorithms, they are less likely to cause complication in design optimization. Among the zero order algorithms, which require only the values of the objective function for given values of design variables, there are stochastic global search algorithms like simulated annealing and genetic algorithm and deterministic local search algorithms like Nelder-Mead and Powell's method. Structural optimization problems may contain many locally optimum designs including the best design together with high - cost local optimum designs. Stochastic algorithms have the advantage of being able to locate the globally optimum design starting from any initial configuration; but they usually require tens of thousands of iterations to converge. Considering that a nonlinear FEA is conducted to analyze the welded plates in the present study and many spot welds are used in typical industrial applications, stochastic algorithms are not found to be practicable for the present problem with today's computational capabilities. Powell's method is known to have some convergence problems. On the other hand, Nelder-Mead is a robust algorithm, eventually converging to a local optimum. For this reason, Nelder-Mead is chosen as the search algorithm. The optimization process is repeated many times starting from different arbitrary configurations for each problem to avoid locally optimum designs with a high objective function value.

4.3. Finite element analysis

Fatigue cracks generally occur at the nugget edge on the inner surface and propagate to the outer surface of the plate (Fig. 2), where a multiaxial stress state develops, and due to high stress concentration, nonlinear deformation and yielding may occur. In order to accurately determine the stress and strain states developed in the structure around the spot weld nugget for a reliable fatigue strength assessment, a nonlinear analysis was carried out using commercial FEA software, ANSYS. The residual stresses arising from non-uniform plastic deformations during loading were taken into account. A kinematic hardening material model (KINH) was used to simulate the nonlinear stress-strain relation. This model includes the Besseling formulation, which takes into account the Bauschinger effect in cyclic loading. The base metal was modeled using 3D 10-node tetrahedral solid elements, SOLID92. This element has plasticity, stress stiffening, large deflection, and large strain capabilities. The spot weld nugget was modeled using a two-node beam element, BEAM188, which has six degrees of freedom at each node. Because this element is based on Timoshenko beam theory, shear deformation effects are included, which are especially important for short beams. Contact elements were defined on the interfaces between the plates around the spot welds. Relative rotation of the region around the spot welds with respect to the beam element is prevented through constraint equations.

In order to obtain an appropriate mesh structure that may enable accurate calculation of the stress state, a convergence analysis was carried out for the element size. Because high stress concentration occurs in the vicinities of the spot welds, much

smaller elements were used within and around the spot-welds in comparison to that of the base metal. Fig. 7 shows the finite element mesh of two spot-welded joint as an example. As the positions of the spot welds change during the optimization process, the model is remeshed and refinement is introduced at the new positions of the welds. The number of elements ranges between 30,000 and 55,000 depending on the number of spot welds in the joint. The details of the FEA and the material properties used in the models can be found in references [1,7].

4.3.1. Boundary conditions

The boundary conditions in the FEA model are shown in Figs. 7–9. In one loading case, displacements and rotations in all degrees of freedom are fixed at one end; the other end is subjected to uniformly distributed in-plane load cycle between 1 and 3 kN in the x-direction, while the movement is prevented in other degrees of freedom. The boundary conditions for the other loading case are the same except that the right end is not restrained in the y-direction; instead a load is applied fluctuating between 1 and 2 kN.

The cyclic loading is applied in two load steps. First, the load is incrementally increased to its maximum value, F_{max}, and the resulting strain state is obtained. In the second load step, the load is incrementally decreased to its minimum value, F_{min}. In the next load cycles, stresses are assumed to fluctuate between the stress values obtained for the maximum and minimum load levels in the first load cycle. A convergence analysis was also carried out to find an appropriate number of substeps.

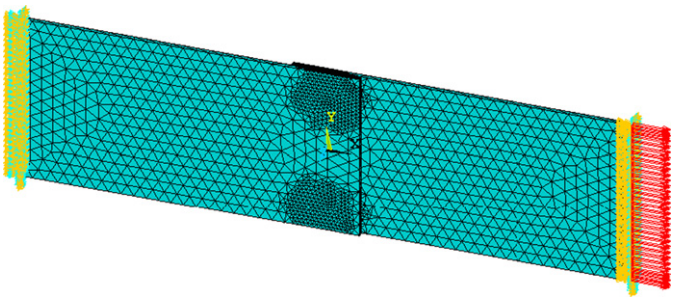

Fig. 7. Finite element model for two spot-welded TS joint.

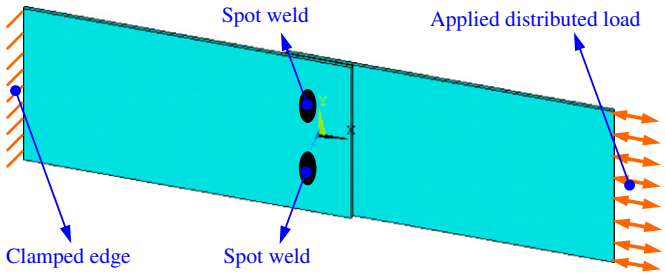

Fig. 8. Boundary conditions of the finite element model for the axial loading case.

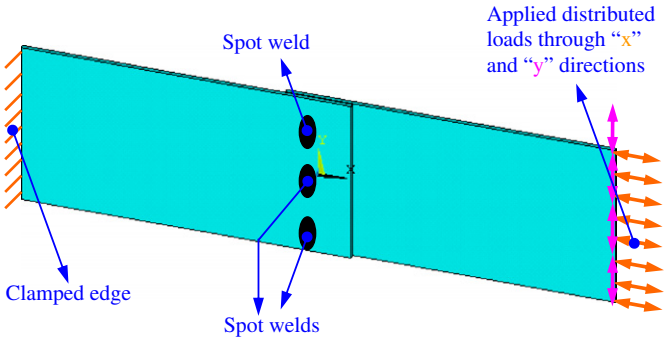

Fig. 9. Boundary conditions of the finite element model for the axial and transverse loading case.

The process of nucleation, growth and joining of micro-cracks is expected to take place in highly stressed regions. Fatigue crack growth is known to occur along planes where the tensile stress takes its maximum value. Hence, the fatigue life calculation (Eq. (2)) is carried out using the stress and strain state in the element at which the maximum tensile stress develops. This element is located at the faying surface in the heat affected zone around the peripheries of the spot welds.

Residual stresses inevitably arise in spot welded structures due to the fact that the metal locally melts and then contracts as it cools down after the current is turned off. Other than this, residual stresses may arise also due to localized plastic deformations around the spot welds after unloading. In this study, residual stresses due to plastic deformation are taken into account; but residual stresses developed during the formation of the spot weld due to thermal effects are assumed not to affect the fatigue life and are not considered in the stress analysis. This assumption is justified, firstly, because there is reasonably well agreement between the measured fatigue life data and the predictions as seen in Figs. 3–5. Secondly, in the previous study [1] a better correlation was obtained via the modified Coffin - Manson model (Eq. (2)), which did not take into account the effect of mean stress, in comparison to Morrow's mean stress model. This implied that the influence of mean stress on fatigue life of spot welds was not significant. No observed effect of mean stress also corroborates our assumption that residual stresses developed during the welding process have little effect on fatigue life since they mainly affect mean stresses rather than alternating stresses.

5. Results and discussions

A computer program was developed using ANSYS parametric design language to implement the optimization algorithm and carry out the structural analyses through finite element method. In the finite element (FE) model, the material properties of DIN 1623 were used. Its engineering stress-strain diagram is given in Fig. 10. The elastic properties of the material are $E=207$ GPa, and $\nu=0.25$ [7]. The material constants used in the fatigue assessment model are given in Table 1. A spot-welded joint is composed of a nugget, heat affected zone (HAZ) (Fig. 1), and base metal in general. Because elastic modulus and Poisson's ratio are not affected by heat treatment, their magnitudes remain the same throughout the

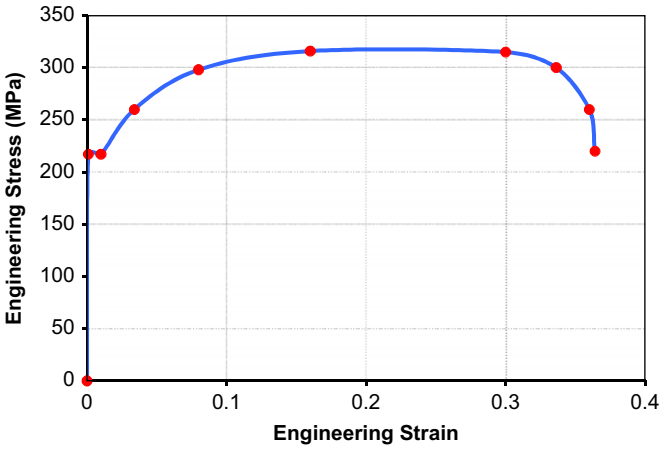

Fig. 10. Engineering stress-strain curve [7].

Table 1
The material constants used in the fatigue assessment model [16].

σ_f'	ε_f'	b	c
499 MPa	0.104	−0.06	−0.4

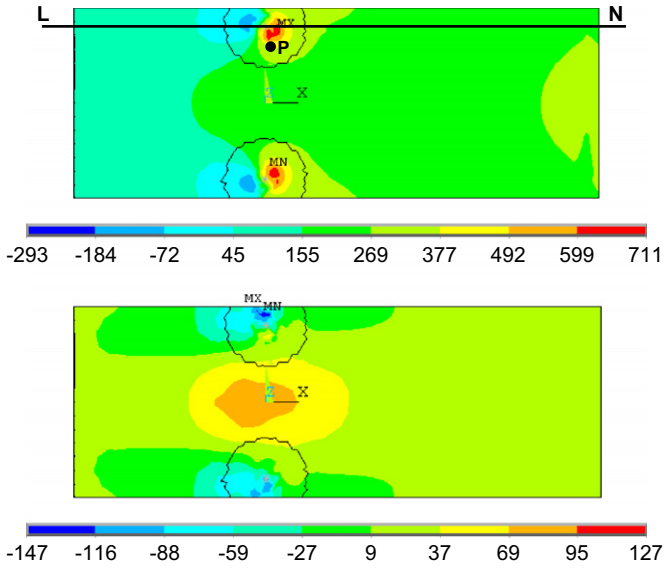

Fig. 11. Distribution of σ_{xx} component of stress (in MPa) on the inner surface of one plate with two spot welds subjected to the maximum axial load (upper figure) and the minimum axial load (lower figure) for the initial design.

specimen despite melting during the formation of the nugget. Although the nonlinear stress-strain relation of the material in and around the nugget is affected during the joining operation, this effect is neglected considering that the steel was not hardened. Because the hardness levels at these locations were measured and found to be close to each other [7], one may assume that there is no significant change in the mechanical properties of the material during welding. The engineering stress-strain curve of the base material (DIN 1623), shown in Fig. 10, is assumed to be valid for the HAZ. Hence, the same material properties are used for both the base material and HAZ in fatigue life calculations. It should also be noted that the homogeneous material assumption is made for the particular material that was chosen for the simulations; but this is not a restriction for the FEA code developed to simulate the mechanical response of the spot weld joints. If the material properties of the heat affected zone are available for a material, the code can use them to account for inhomogeneity around the spot welds.

5.1. Optimization of a joint with two spots under cyclic axial loading

First, a two-spot-welded joint subjected to an axial load cycle with constant load amplitude were optimized in which y coordinate of the spot welds and overlapping length were chosen as design variables. Starting from different initial designs, the optimization process was repeated many times. In one of these trials, the initial coordinates of the spot welds were (0, 16) mm and (0, −16) mm and the overlapping length (ℓ) was 80 mm. Critical stresses developed on the inner surfaces of the plates. Fig. 11 shows the distribution of σ_{xx} component of stress (before optimization) on the inner surface of one of the plates corresponding to the maximum and the minimum loads, respectively. Dashed lines show the boundaries of the contact region around the spot welds. The nuggets caused bending of the plates such that highly localized tensile and compressive stresses above the yield point developed around them. When the load is reduced from its maximum value (3 kN) to its minimum value (1 kN), compressive residual stresses develop at points where the maximum tensile stress develops at full load. The corresponding fatigue life of the joint was calculated as 12,047 cycles. Figs. 12 and 13 show the multiaxial stress distribution along the length of the plate (L-N line in Fig. 11, which contain the maximum normal stress) and through the thickness (through point P in Fig. 11) for the initial design, respectively. In these figure, one may better see the severity of the stress concentration and how the stresses change from tension to compression from one side of the plate to the other due to bending. After 66 iterations, the fatigue life reached to its maximum value, 64,705 cycles, corresponding to the optimal coordinates (0, 11.84) mm, (0, −11.84) mm and optimal overlapping length of 18.48 mm. Nelder-Mead algorithm used n+1 current configurations, n being the number of design variables. Fig. 14 shows the change in the fatigue lives of the best and the worst of the current configurations generated during the optimization process.

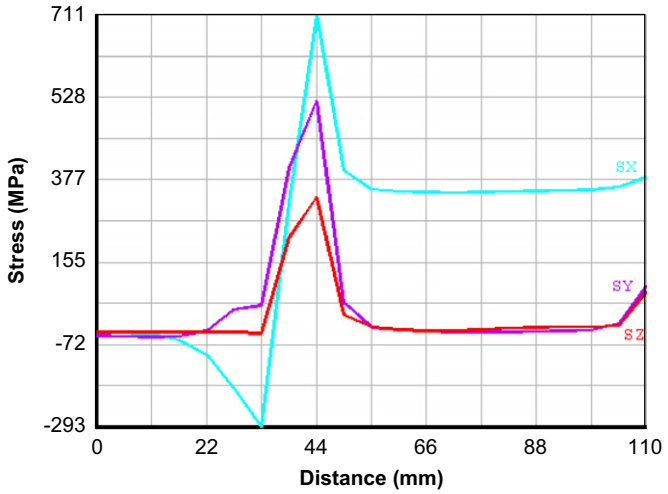

Fig. 12. Distribution of the stress components σ_{xx}, σ_{yy}, and τ_{xy} along the line L-N shown in Fig. 11, which passes through one of the spot welds, for the maximum axial loading condition and for the initial design.

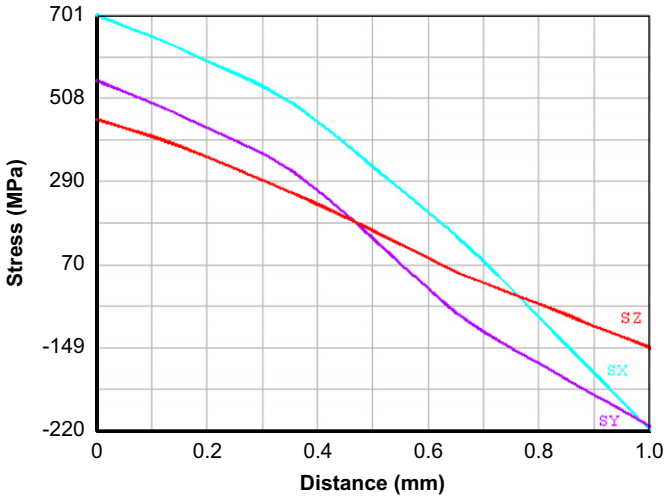

Fig. 13. Distribution of the stress components σ_{xx}, σ_{yy}, and τ_{xy} (in MPa) through the thickness along a line passing through the point P in Fig. 11 for the maximum axial loading condition for the initial design.

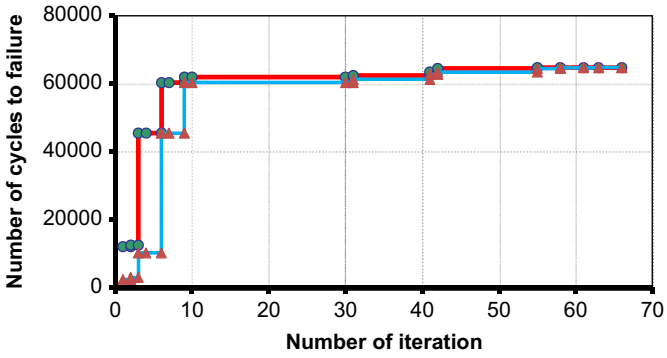

Fig. 14. The change in the fatigue life of the best and worst current configurations generated during the optimization process.

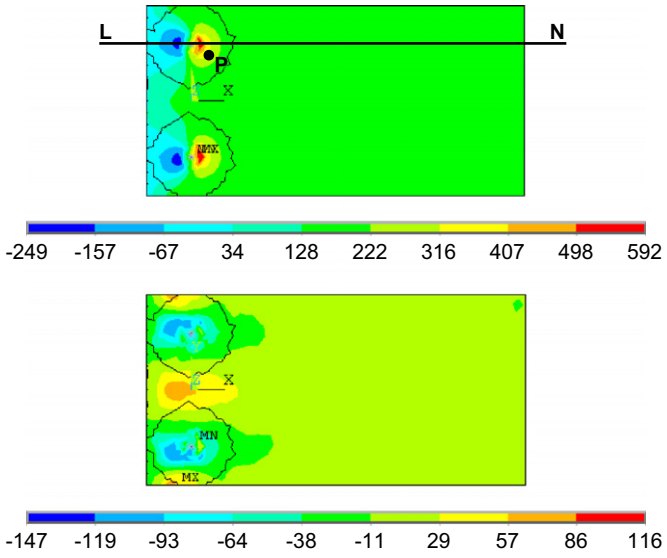

Fig. 15. Distribution of σ_{xx} component of stress (in MPa) on the inner surface of one plate with two spot welds subjected to the maximum axial load (upper figure) and the minimum axial load (lower figure) for the optimized design.

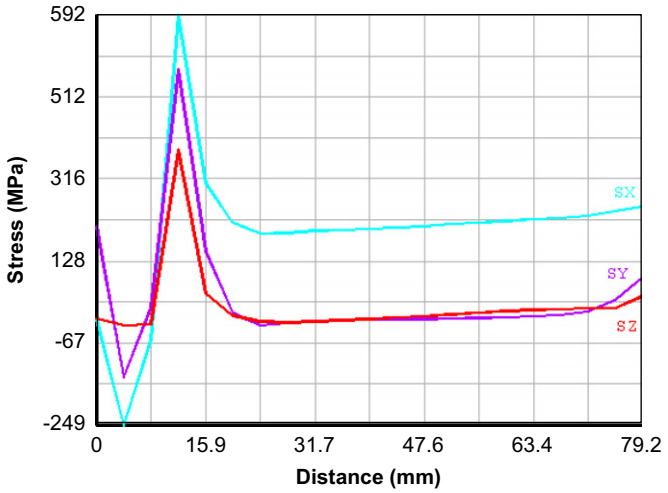

Fig. 16. Distribution of the stress components σ_{xx}, σ_{yy}, and τ_{xy} along the line L-N shown in Fig. 15, which passes through one of the spot welds, for the maximum axial loading condition for the optimized design.

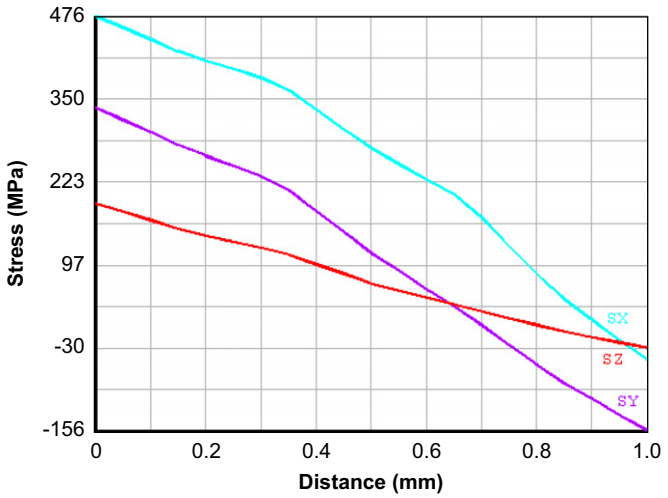

Fig. 17. Distribution of the stress components σ_{xx}, σ_{yy}, and τ_{xy} (in MPa) through the thickness along a line passing through the point P in Fig. 15 for the maximum axial loading condition for the optimized design.

Similar to the other optimization processes, at the initial stages of optimization, considerable improvement in the objective function value is achieved, while in the later stages, less pronounced improvement occurs. Initially, the difference between the best and the worst configurations is large; this becomes smaller and smaller during the optimization. Fig. 15 shows the resulting stress distributions in the optimally designed plate. As seen in Figs. 11 and 15, stress concentration is considerably reduced through the optimization. Figs. 16 and 17 show the multiaxial stress distribution in the optimized plate, respectively. As seen in Figs. 11–17, the highest stresses develop on the faying surface around the periphery of the spot welds. This conforms to the fatigue crack initiation locations observed in the experiments [7]. In the optimum design, the overlapping length of the plates is also significantly reduced.

Table 2 lists some of the optimization results obtained starting from different initial configurations. There are a number of near global optimums and worse local optimums. Because repeated optimization runs yield similar configurations and they group around a few local optimums, repeated use of a local search algorithm may be considered to be sufficient to find the best joint design. In the optimum configuration, the distance between the centers of the spots to the edges is about 8 mm, while the distance between them is about 24 mm. This means that the constraints given in Eqs. Eq. (6) and (7) are not active considering that the diameter is 4 mm. The overlapping length, ℓ, is about 20 mm. Then Eq. (5) is also not active. This suggests that the industrial guideline that the distance between an edge and spot weld center should be greater than one spot weld diameter is non-conservative. If metal fatigue is the critical failure mode, it should be about 1.5–2.0 times the diameter according to our results.

5.2. *Optimization of a joint with two spots under cyclic axial and transverse loading*

In this case, a joint with two spot welds subjected to both axial and transverse load cycles with constant load amplitude (Fig. 18) was optimized (Fig. 19) in which x and y coordinates of the spot welds and overlapping length, ℓ, were chosen as design variables. Table 3 lists some of the optimization results obtained starting from different initial configurations. In one of the optimization runs, the initial coordinates of the spot welds were (15, 6) mm and (−10, −6.5) mm and the overlapping length was 90 mm. Fig. 18 shows the distribution of σ_{xx} component of stress for the initial design. The corresponding fatigue life of the joint was 4428 cycles. After 117 iterations, 19,865 cycles of fatigue life were obtained

Table 2
Optimization results for a joint with two spots under cyclic axial loading. ℓ is the overlapping length, y is the y-coordinate of the upper spot.

Trial no.	Initial coordinates (mm) for simplex						Optimized values		Fatigue life (cycles)
	First point		Second point		Third point				
	y	ℓ	y	ℓ	y	ℓ	y	ℓ	N_f
1	16	80	15	90	14	100	11.84	18.48	64,705
2	6	34	5	22	8	40	13.62	21.51	64,650
3	17	90	10	80	13	100	13.35	20.25	62,903
4	18	50	15	70	13	60	13.96	20.68	62,256
5	9	64	9	102	14	60	13.68	22.63	61,950
6	14	76	14	98	6	54	14.05	19.96	60,032
7	18	10	17	12	16	14	13.52	20.58	45,620
8	15	16	14	18	13	20	13.68	20.69	41,259
9	12	22	11	24	10	26	11.01	25.23	28,596
10	8	36	9	38	7	34	9.91	40.45	26,956

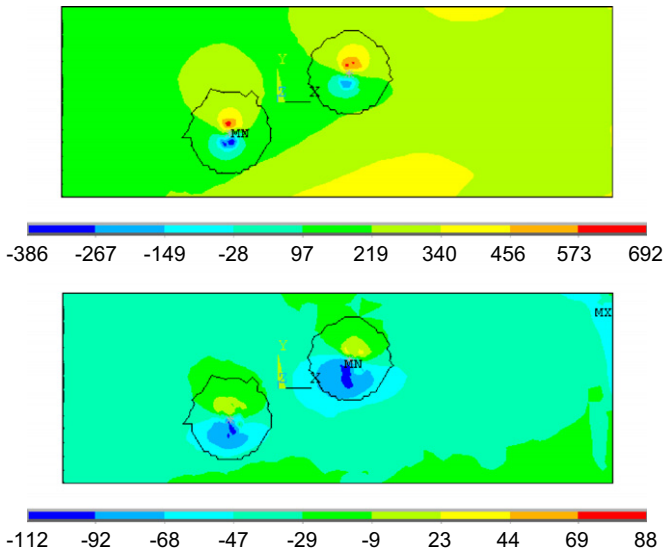

Fig. 18. Distribution of σ_{xx} component of stress (in MPa) on the inner surface of one plate with two spot welds subjected to the maximum axial and transverse loads (upper figure) and the minimum axial and transverse loads (lower figure) for the initial design.

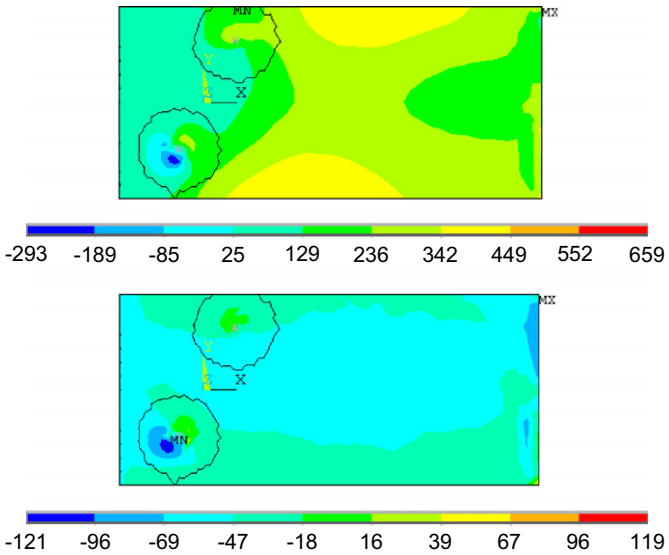

Fig. 19. Distribution of σ_{xx} component of stress (in MPa) on the inner surface of one plate with two spot welds subjected to the maximum axial and transverse loads (upper figure) and the minimum axial and transverse loads (lower figure) for the optimized design.

corresponding to the optimal coordinates (6.62, 12.98) mm, (−5.1, −9.71) mm and optimal overlapping length of 35.06 mm. Fig. 19 shows the resulting stress distributions on the optimally design plate. The resulting optimal positions are not compatible with the industrial practice. The algorithm does not place the spots symmetrically under transverse loads. The distance to the edges in the optimal configuration is about 1.5 times the diameter. In this case, in order to find the global optimum design, the optimization process was repeated 14 times starting from different points.

5.3. Optimization of a joint with three spots under cyclic axial loading

In this case, three-spot-welded joints subjected to an axial load cycle with constant load amplitude were optimized. One of the spot welds was positioned at the center of the joint and its location was not changed during the optimization while the others were free to move. Table 4 lists some of the optimization results obtained starting from different initial configurations.

In one of the trials, the initial coordinates of the spot welds were (21, 15) mm, (0, 0) mm and (11, −12) mm and overlapping length (ℓ) was 110 mm. Fig. 20 shows the distribution of σ_{xx} component of stress. The corresponding fatigue life of the joint was 425,791 cycles. After 69 iterations, a fatigue life of 1,391,655 cycles was obtained for the optimal coordinates of (0, 14.35) mm, (0, 0) mm, and (0.41, −14.26) mm and optimal overlapping length of 16.50 mm. Although symmetry is not imposed as a constraint, the algorithm almost symmetrically places the spots under axial loading. Fig. 21 shows the resulting true stress distributions on the optimally design plate. The number of spot welds significantly affects the fatigue strength. Using one more spot weld increases the fatigue life about 20 times.

5.4. Optimization of a joint with three spots under cyclic axial and transverse loading

In this case, a joint with three spot welds subjected to both an axial and a transverse load cycles with constant load amplitude was optimized. Also for this problem, centrally positioned spot weld was fixed and the positions of the other two were optimized. In one of the optimization runs, initial coordinates of the spot welds were (−14, 13) mm, (0, 0) mm and (13, −14) mm and overlapping length (ℓ) was 100 mm. Fig. 22 shows the distribution of σ_{xx} component of stress for the initial design corresponding to the maximum load. The corresponding fatigue life of the joint was 6168

Table 3
Optimization results for a joint with two spots under cyclic axial and transverse loading. x_i and y_i are the coordinates of spot weld i.

	$x1$	$y1$	$x2$	$y2$	ℓ		$x1$	$y1$	$x2$	$y2$	ℓ
Trial no. 1						*Trial no. 2*					
First point	15	6	−10	−6.5	90	First point	15	2	−15	−1	80
Second point	10	7	−14	−4	75	Second point	14	5	−14	−4	75
Third point	5	8	−13	−7	70	Third point	13	8	−13	−7	70
Fourth point	15	8	−13	−7	70	Fourth point	12	11	−13	−7	70
Fifth point	10	7	−14	−4.5	75	Fifth point	11	2	−14	−4	75
Sixth point	5	6	−15	−1	80	Sixth point	10	6	−15	−1	80
Optimized values	6.62	12.98	−5.1	−9.71	35.06	Optimized values	5.9	12.12	−4.76	−11.1	39.8
Fatigue life (cycles)			19,865			Fatigue life (cycles)			18,970		
Trial no. 3						*Trial no. 4*					
First point	15	2	−3	−8	80	First point	5	2	−1	−8	80
Second point	14	5	−6	−4	90	Second point	5	7	−3	−4	90
Third point	13	8	−9	−9	70	Third point	5	7	−1	−7	75
Fourth point	12	11	−12	−7	90	Fourth point	6	4	−1	−7	90
Fifth point	11	2	−15	−4	100	Fifth point	7	5	−10	−10	45
Sixth point	10	6	−4	−10	110	Sixth point	7	5	−4	−2	60
Optimized values	6.32	12.1	−4.6	−10.2	41.5	Optimized values	6.3	11.4	−4.4	−10.6	43.6
Fatigue life (cycles)			18,870			Fatigue life (cycles)			18,290		
Trial no. 5						*Trial no. 6*					
First point	3	2	−10	−5	45	First point	3	9	−7	−11	80
Second point	4	7	−9	−6	50	Second point	9	12	−8	−12	90
Third point	7	3	−8	−7	55	Third point	5	5	−9	−13	100
Fourth point	8	9	−7	−8	60	Fourth point	7	13	−10	−14	80
Fifth point	9	5	−6	−9	65	Fifth point	3	9	−10	−15	70
Sixth point	9	2	−5	−10	70	Sixth point	8	10	−11	−16	60
Optimized values	7.2	13.4	−6.9	−11.1	36.7	Optimized values	5.9	13	−6.6	−12.3	47.3
Fatigue life (cycles)			17,570			Fatigue life (cycles)			16,940		

Table 4
Optimization results for a joint with three spots under cyclic axial loading.

	$x1$	$y1$	$x3$	$y3$	ℓ		$x1$	$y1$	$x3$	$y3$	ℓ
Trial no 1						*Trial no 2*					
First point	21	15	11	−12	110	First point	12	15	−15	−1	100
Second point	5	19	14	−20	99	Second point	12	12	−13	−20	75
Third point	9	18	13	−12	78	Third point	12	11	−14	−3	50
Fourth point	12	17	12	−13	56	Fourth point	20	10	12	−13	25
Fifth point	16	16	11	−14	89	Fifth point	20	6	11	−5	50
Sixth point	20	15	10	−15	57	Sixth point	20	17	10	−15	75
Optimized values	0	14.4	0.4	−14.3	16.5	Optimized values	0	15.2	0	−15.5	20.2
Fatigue life (cycles)			1,391,655			Fatigue life (cycles)			1,245,490		
Trial no. 3						*Trial no. 4*					
First point	5	6	−15	−1	110	First point	0	10	−15	−7	30
Second point	6	12	6	−3	60	Second point	10	8	6	−3	35
Third point	7	8	−14	−3	100	Third point	0	8	−14	−7	40
Fourth point	8	10	12	−13	70	Fourth point	5	10	0	−13	45
Fifth point	9	6	−11	−12	90	Fifth point	0	7	−11	−1	50
Sixth point	12	17	10	−15	80	Sixth point	10	7	0	−15	55
Optimized values	0.1	16.6	0	−15.2	20	Optimized values	1.1	17.4	−1	−16.5	31
Fatigue life (cycles)			1,217,590			Fatigue life (cycles)			1,149,674		
Trial no. 5						*Trial no. 6*					
First point	15	5	−1	−10	20	First point	0	10	−13	−18	40
Second point	14	5	−10	−1	40	Second point	1	15	−10	−1	50
Third point	13	0	13	−12	50	Third point	5	18	13	−15	60
Fourth point	12	6	12	−2	70	Fourth point	12	6	12	−7	100
Fifth point	11	3	0	−14	87	Fifth point	9	3	−7	−13	90
Sixth point	10	9	10	−3	57	Sixth point	4	9	10	−2	60
Optimized values	1.1	13.4	−1.4	−15	27	Optimized values	0.8	14.9	−0.5	−16.3	29
Fatigue life (cycles)			1,145,233			Fatigue life (cycles)			1,110,566		

cycles. After 73 iterations, a fatigue life of 168,356 cycles was obtained for the optimal coordinates (13.51, 12.12) mm, (0, 0) mm, and (−13.25, −14.24) mm and optimal overlapping length of 65.58 mm. Fig. 23 shows the resulting maximum stress distributions on the optimally design plate. In the optimal configuration, the spot welds are not symmetrically placed because of the transverse loads.

In this study, experimental verification of the optimized spot-weld geometry was not attempted because of the difficulties in realizing the experimental conditions. In order to experimentally

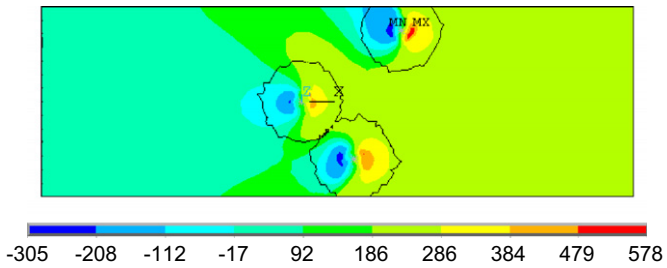

Fig. 20. Distribution of σ_{xx} component of stress (in MPa) on the inner surface of one plate with three spot welds subjected to the maximum axial load for the initial design.

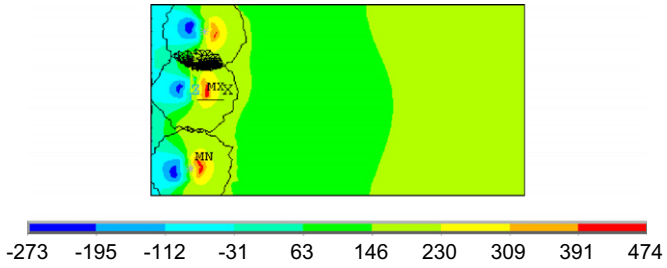

Fig. 21. Distribution of σ_{xx} component of stress (in MPa) on the inner surface of one plate with three spot welds subjected to the maximum axial load for the optimized design.

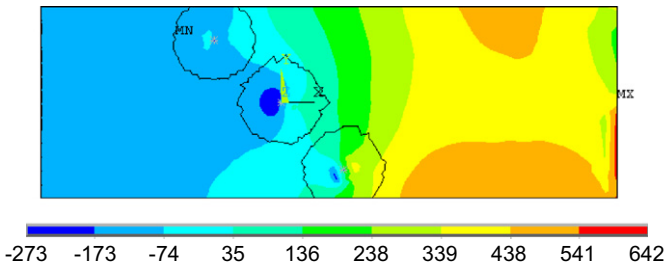

Fig. 22. Distribution of σ_{xx} component of stress (in MPa) on the inner surface of one plate with three spot welds subjected to the maximum axial and transverse loads for the initial design.

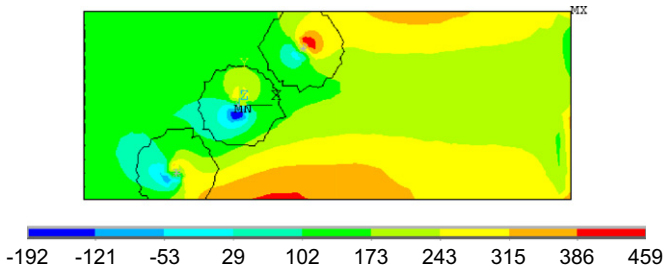

Fig. 23. Distribution of σ_{xx} component of stress (in MPa) on the inner surface of one plate with three spot welds subjected to the maximum axial and transverse loads for the optimized design.

validate the optimized geometry, spot welds should be generated at the optimized positions precisely; axial and transverse loads should be applied precisely and their load cycles should be synchronous; a special testing machine and a special experimental set-up should be constructed unlike the standard experiments. For these reasons, the fatigue assessment model was verified by comparing its predictions with the experimental data obtained through standard tests as in Figs. 3–5.

6. Conclusions

In this study, a design optimization procedure is proposed to maximize the fatigue life of spot weld joints. This procedure was applied to a number of problems in order to check the effectiveness of the algorithm. Because a local search algorithm, Nelder & Mead, was used to determine the optimal positions of spots and optimal overlapping length, the optimization process was repeated many times starting from different configurations and the optimal design with the highest fatigue life was presumed to be the globally optimum design. Since the results show that a limited number of local minima exist, use of a local search algorithm is more appropriate instead of a computationally expensive global optimization algorithm. However, if the design of plates joined with many spot welds is to be optimized, many local optimum designs may exist. In that case, use of a global search algorithm may be justified to find the globally optimal design. The optimization procedure developed in this study can easily be adapted to other search algorithms.

In the optimization procedure, penalty functions were introduced to prevent the spots getting close to each other and the boundaries of the plates. With the increased number of spot welds the complexity of the optimization problem increases as well as the possibility of improvement. Significant differences in fatigue life may exist between optimal and non-optimal designs.

As shown in the previous study [1], the predictions of the fatigue assessment model correlate well with the fatigue data for the other types of specimens, modified tensile - shear, coach peel, and modified coach peel. Therefore, the analysis method and the design optimization procedure are also applicable to spot welded plates with different geometries.

Fatigue life of spot welded joints, which depends on the stress and strain states around the spot welds, is a very complex function of the spot-weld positions, even in the case of two spots. Even an experienced designer may not guess the optimal design in many cases. This means that simple rules of thumb for optimal designs are not viable.

Acknowledgements

This paper is based on the work supported by TUBITAK, The Scientific and Technological Research Council of Turkey, with the code number 106M301.

References

[1] A.H. Ertas, F.O. Sonmez, A parametric study on fatigue strength of spot-weld joints, Fatigue & Fracture of Engineering Materials & Structures 31 (2008) 766–776.
[2] Y.J. Chao, Failure mode of spot welds: interfacial versus pullout, Sci Technol Weld Joi 8 (2003) 133–137.
[3] Y. Zhang, D. Taylor, Optimization of spot-welded structures, Finite Elem Anal Des 37 (2001) 1013–1022.
[4] S.W. Chae, K.Y. Kwon, T.S. Lee, An optimal design system for spot welding locations, Finite Elem Anal Des 38 (2002) 277–294.
[5] Y. Rui, R.J. Yang, C.J. Chen, H. Agrawal, Fatigue optimization of spot welds, Body Des Eng. IBEC 96 (1996) 68–72.
[6] W. Liangsheng, K.B. Prodyot, J.P. Leiva, Design optimization of automobile welds, Int J Vehicle Des 31 (2003) 377–391.
[7] A.H. Ertas, O. Vardar, F.O. Sonmez, Z. Solim, Measurement and assessment of fatigue life of spot-weld joints, J Eng Mater-T ASME, 131, , 2009 Article Number-011011.
[8] J.A. Newman, N.E. Dowling, A crack growth approach to life prediction of spot-welded lap joints, Fatigue Fract Eng M 21 (1998) 1123–1132.
[9] Ertas A.H. Fatigue Behavior of Spot Welds. M.Sc Thesis, Bogazici University, 2004.
[10] Pan N. Fatigue Life Study of Spot welds. Ph.D. Thesis, Stanford University, 2000.
[11] Y.R. Kan, Fatigue resistance of spot welds-an analytical study, Met Eng Q 16 (1976) 26–36.

[12] Gero B.M. Acousto-Ultrasonic Evaluation of Cyclic Fatigue of Spot Welded Structures. M. Sc. Thesis, Virginia Polytechnic Institute and State University, 1997.
[13] Davidon J.A. A review of the fatigue properties of spot-welded sheet steels. SAE International Congress and Exposition, Detroit, MI, 1982.
[14] A. Gean, A. Westgate, J.C. Kucza, J.C. Ehrstrom, Static and fatigue behavior of spot-welded 5182-O Aluminum ally sheet, Weld J 78 (1999) 90–96.
[15] S. Suresh, Fatigue of Materials, Cambridge University Press, 2004.
[16] Stephens R.I., Fatemi A., Stephens R.R., Fuchs H.O. Metal Fatigue in Engineering, 2000.
[17] N. Pan, S. Sheppard, Spot welds fatigue life prediction with cyclic strain range, Int J Fatigue 24 (2002) 519–528.
[18] R.T. Haftka, Z. Gurdal, Elements of Structural Optimization, Kluwer Academic Publishers, 1992.
[19] Rao S.S. Engineering Optimization: Theory and Practice, 1996.